Available online at www.sciencedirect.com
ScienceDirect
Fisheries Research 86 (2007) 42–57
FISHERIES RESEARCH
www.elsevier.com/locate/fishres

Population parameters of the smooth lantern shark, *Etmopterus pusillus*, in southern Portugal (NE Atlantic)

Rui Coelho *, Karim Erzini

Universidade do Algarve, FCMA/CCMAR, Campus de Gambelas, 8005-139 Faro, Portugal

Received 20 December 2006; received in revised form 19 April 2007; accepted 20 April 2007

Abstract

Etmopterus pusillus is a deep water lantern shark with a widespread global distribution that is caught in large quantities in some areas, but is usually discarded due to the low commercial value. In this work, the population biology was studied and life history parameters determined for the first time in this species. Age was estimated from sections of the second dorsal spine and validated by marginal increment analysis. Males attained a maximum age of 13 years, while 17-year-old females were found. Several growth models were fitted and compared for both size and weight at age data, showing that even though this is a small sized species, it has a relatively slow growth rate. This species matures late and at a relatively large size: at 86.81% and 79.40% of the maximum observed sizes and at 58.02% and 54.40% of the maximum observed ages for males and females, respectively. It has a low fecundity, with a mean ovarian fecundity of 10.44 oocytes per reproductive cycle. The estimated parameters indicate that this species has a vulnerable life cycle, typical of deep water squalid sharks. Given the high fishing pressures that it is suffering in the NE Atlantic, the smooth lantern shark may be in danger of severe declines in the near future.

Keywords: Age and growth; Elasmobranch; Fecundity; Fisheries management; Population dynamics; Reproduction; Species conservation

1. Introduction

The smooth lantern shark, *Etmopterus pusillus* is a small sized, globally widespread, deep water squalid shark. In the western Atlantic it has been recorded in the northern area of the Gulf of Mexico and between southern Brazil and Argentina (Compagno, 1984). In the eastern Atlantic it has been recorded from Portugal (Saldanha, 1997) to Namibia. In the western Indian Ocean it has been described for South Africa and in the western Pacific in Japan (Compagno, 1984). This species lives mainly in the continental and insular shelves and upper slopes, at depths from 274 to 1000 m, but has also been described in oceanic waters, between Argentina and South Africa (Compagno, 1984).

The family Etmopteridae is the largest squaloid shark family, with more than 50 species in 5 genera. The *Etmopterus* genus is the most speciose genus in this family, currently with 31 valid species (Compagno et al., 2005). Most of the species in this genus are either endemic or very limited in their distribution, and *E. pusillus* is one of the few with a cosmopolitan distribution (Compagno et al., 2005). However, it is particularly abundant only in some areas such as off the south and southwestern coasts of Portugal. Here, this species, along with *Etmopterus spinax*, comprise the two most abundant lantern sharks (Coelho et al., 2005).

In Portugal, *E. pusillus* is commonly caught as by-catch and discarded by several deep water fisheries that operate in the area, namely the deep bottom trawl fishery that targets Norway lobster, *Nephrops norvegicus*, deepwater rose shrimp, *Parapenaeus longirostris*, and red shrimp, *Aristeus antennatus* (Monteiro et al., 2001) and the deep water longline fishery that targets wreckfish, *Polyprion americanus*, European-conger, *Conger conger*, and European hake, *Merluccius merluccius* (Coelho et al., 2005). However, even though *E. pusillus* is caught in large quantities, it has a very low or no commercial value and is therefore usually discarded (Monteiro et al., 2001; Coelho et al., 2005). Therefore, this species is never landed and is never accounted for in the official fisheries statistics, limiting the availability of data for monitoring its fisheries mortality and assessing its population status.

Although *E. pusillus* is widespread, little biological information exists on this species. Coelho and Erzini (2005) report

* Corresponding author. Tel.: +351 289 800 900; fax: +351 289 818 353.
E-mail address: rpcoelho@ualg.pt (R. Coelho).
URL: www.ualg.pt/fcma/cfrg (R. Coelho).

0165-7836/$ – see front matter © 2007 Elsevier B.V. All rights reserved.
doi:10.1016/j.fishres.2007.04.006

that this is an aplacental viviparous species, and present preliminary lengths-at-maturity, but no other biological information is available. We believe that this is the first study that focuses on detailed life history parameters of this species.

Given the relatively high levels of fishing mortality that this species is currently suffering and that this is a deep water squalid shark, a family of sharks generally characterized by very vulnerable life cycles, with very slow growth rates, late maturities and low reproductive potential (Fowler et al., 2005), there is an urgent need for biological studies of this species. The objectives were to study various aspects of the population biology of *E. pusillus*, especially growth, maturity and fecundity. The data presented here will be useful for modelling purposes (e.g. risk analysis), for monitoring this population's evolution in the future and may serve as a basis for comparison with other studies on this species in other areas.

2. Materials and methods

2.1. Biological sample

Specimens were caught on a monthly basis, from February 2003 to June 2004, except for March 2003, as by-catch of commercial fishing vessels, namely deep water trawlers and deep water longliners. The commercial longliners usually operated on rocky bottoms to catch demersal bony fishes such as *P. americanus* and *C. conger*, while the commercial trawlers operated on muddy and sandy bottoms, targetting crustaceans such as *N. norvegicus*, *P. longirostris* and *A. antennatus*. Additionally, specimens were obtained from the Portuguese Fisheries Institute (INIAP—IPIMAR) deep water trawl research cruise during the summer of 2003. Samples came from fishing that took place at depths from 245 to 745 m (Fig. 1).

All specimens caught were brought to the laboratory where a series of external body measurements were taken to the nearest lower millimetre, namely the total length (TL), measured in a straight line from the tip of the snout to the tip of the caudal fin in its natural position, the fork length (FL), measured form the tip of the snout to the caudal fin fork, the pre-caudal length (PCL), measured from the tip of the snout to the beginning of the upper lobe of the caudal fin and the body girth (GIR) measured around the body at its widest area. Total weight (W) and eviscerated weight (W_{ev}) were recorded to the nearest centigram. After dissection, the gonads and the liver were weighed to the nearest centigram. Additionally, electronic callipers were used to measure the inner clasper lengths in males, from the vent opening

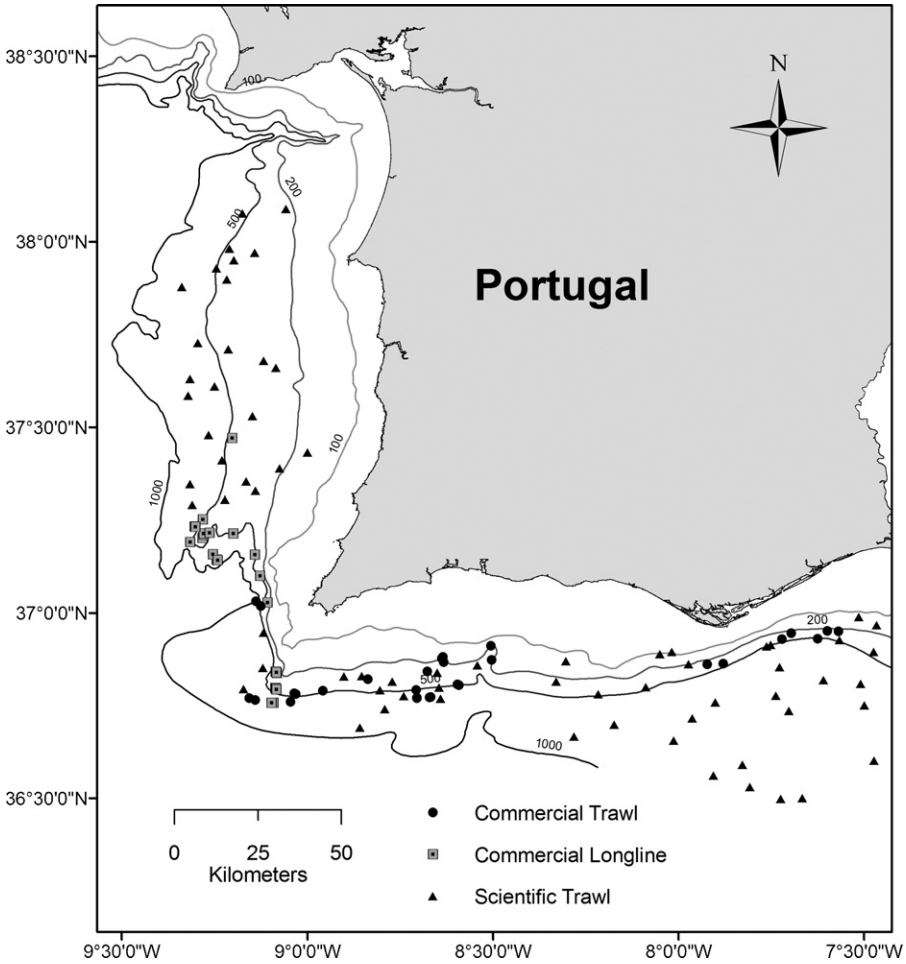

Fig. 1. Map of the south and southwestern coasts of Portugal with the location of the coastline, the bathymetric lines (100, 200, 500 and 1000 m depths), the commercial fishing operations and the research survey tows. Bathymetric lines and coastline adapted from "Atlas do Ambiente Digital—Instituto do Ambiente".

to the tip of the claspers, and the uterus diameter of females in its widest area, to the nearest 0.01 mm. The diameter of ripe oocytes in mature females and the length and weight of embryos in pregnant females were also measured, using a digital caliper with 0.01 mm precision and a digital scale with 0.01 g precision.

2.2. Morphometric relationships

The relationships between the explanatory variable TL (in cm) and each of the dependant variables FL, PCL and GIR (in cm) without any data transformation, and between the explanatory variable TL and the dependant variables W and W_{ev} (in g) with natural logarithm transformed data were explored by linear regression. Standard errors were calculated for all the estimated parameters, along with the coefficient of determination (r^2) of each regression. Linear regressions were carried out for males and females separately, and analysis of covariance (ANCOVA), using TL as the covariate, used for comparing the two sexes (homogeneity of the regressions).

2.3. Age estimation and validation

Linear regression was used to assess if there were relationships between specimen growth and dorsal spines growth, an assumption needing verification if age is to be determined in these structures. Linear models were fitted with TL (cm) as the explanatory variable and various variables representing the growth of both the first and the second dorsal spines, namely total spine length (TSL, in mm), measured from the spine tip to the anterior side of the spine base and the spine base width (SBW, in mm), measured as the diameter of the spine at its base (Clarke and Irvine, 2006). Linear regression was also used to explore the relationship between natural logarithm transformed TL and spine weight (SW, in mg). Standard errors were calculated for all the estimated parameters and r^2 values determined. Linear regressions were carried out for males and females separately, with analysis of covariance (ANCOVA), using TL as the covariate for comparing the two sexes (homogeneity of the regressions). All spine measurements were taken with digital calipers with 0.01 mm precision and weights recorded using electronic precision (0.1 mg) scales.

Age was estimated by direct counting of the bands formed in the inner dentine layer of the second dorsal spines. A band was defined as a pair made by an opaque and a hyaline band. The spines were initially cleaned by removing most of the organic tissue with scalpels and scissors. After, the spines were immersed in a sodium hypochlorite (10%) solution, between 2 and 10 min, depending on the size of the structure and until all organic tissue was cleaned. The spines were then rinsed in tap water for 1 min and left immersed in distilled water for 30 min to remove all traces of sodium hypochlorite. The cleaned spines were then stored dry until ready to be processed.

Once dry, the spines were embedded in epoxy resin, in individual plastic moulds. After a 24 h period for complete drying of the epoxy, these moulds were placed in a Buehler Isomet low speed sawing machine using a series 15LC diamond blade to cut three transverse 500 μm sections. Spines were sectioned on the exterior spine region (Irvine et al., 2006a), with the distance of the section to the spine tip varying with spine length. The sections were mounted in microscope glass slides with DPX, and observed in a Zeiss Axiolab binocular microscope with 100× amplification under transmitted white light.

The sharpest section of each specimen was microphotographed with a digital Canon G2 photographic machine mounted in the microscope. All photographs were taken in the aperture priority mode, with this value set manually to the lowest possible aperture (highest F-value, in this case F8.0), to increase the depth of field and decrease the possibility of blurring the photographs. To reduce photo noise, the ISO value was set manually to ISO50 and a manual light exposition compensation of −2/3 EV was set to compensate for possible over-exposure.

All photos were processed and analyzed in the Image Pro Plus 4.5 software. Measurements of the spine radius in the area where the bands were observed were taken and linear regressions established. These regressions were carried for each sex separately and compared with ANCOVA, using TL as the covariate.

Preliminary tests were made on vertebrae to assess their possible use for age confirmation, but given that no bands were visible, even after using the alizarin red S band enhancing technique (LaMarca, 1966), no further processing or analysis of these structures was carried out.

Age was estimated by a single reader who made three independent readings of each structure. To reduce possible sources of bias, these readings took place at least 1 month apart and no information regarding specimen characteristics or previous readings was available during each reading. An age class was only attributed to a specimen if at least two of the three age estimations were concordant.

The precision of the age estimates, defined as the reproducibility of repeated measurements on a given structure (Campana, 2001) was determined by several different techniques. The percent agreement, a technique that determines the percentage of age estimations that agree entirely, that agree within ±1, ±2, ±3 years and so on was used. Given that this technique is dependant on the age estimate, meaning that similar values of percent agreement can have different meanings depending on the range of the age estimates, alternative techniques were also used, namely the average percent error (APE) defined by Beamish and Fournier (1981) and the coefficient of variation (CV) and the index of precision (D) defined by Chang (1982).

The periodicity of the formation of band patterns was validated by using the relative marginal increment analysis, expressed as:

$$\mathrm{MIR} = \frac{R - R_n}{R_n - R_{n-1}}$$

where MIR is the marginal increment ratio, R the radius of the structure, R_n the distance to the outer edge of the last complete band and R_{n-1} is the distance to the outer edge of the next-to-last complete band.

The monthly evolution of the mean MIR was plotted to determine trends in band formation throughout the year. An analysis of variance (ANOVA) was used to test for differences in the

MIR values along the year and the multiple comparisons Tukey pairwise test used to assess differences between pairs of months.

2.4. Growth modelling

Modelling of growth in length was based on four relatively commonly used models, namely the Von Bertalanffy Growth Function (VBGF), a modified version of the VBGF with known size at birth, the Gompertz model and the logistic equation.

The VBGF is one of the most used models to explain fish growth, that can also be applied to other organisms such as cephalopods. The principle underlying this model is that growth rate of fishes tends to decrease linearly with size and it can be expressed as:

$$L_t = L_{inf}(1 - e^{-k(t-t_0)})$$

where L_t is the total length at age t, L_{inf} the maximum asymptotic length, k the growth coefficient and t_0 is the theoretical age when $L_t = 0$.

As an alternative to the traditional VBGF, a model with a fixed intercept of the length axis (known size at birth (L_0)) was used:

$$L_t = L_{inf}(1 - b\,e^{-kt})$$

where $b = (L_{inf} - L_0)/L_{inf}$ and L_0 is the size at birth, that in this species was estimated to be 12.8 cm TL (S.D. = 0.6 cm; $n = 5$), based on observations of totally formed embryos present in late term (stage 6) pregnant females.

The Gompertz growth model is a sigmoidal growth curve that assumes an exponential decrease of the growth rate with size and can be expressed as:

$$L_t = L_{inf}\, e^{-e^{(-g(t-t_0))}}$$

where g is the Gompertz growth coefficient.

The logistic equation can be expressed as:

$$L_t = \frac{L_{inf}}{(1 + ((L_{inf} - L_0)/L_0)(e^{(-rt)}))}$$

where L_0 is the theoretical length at birth and r is the logistic growth coefficient.

Weight-at-age data were modelled using the VBGF and the Gompertz model. The VBGF used with weight data can be expressed as:

$$W_t = W_{inf}(1 - e^{-k(t-t_0)^b})$$

where W_t is the total weight at age t, W_{inf} the maximum asymptotic weight and b is the allometric growth coefficient from the TL-W relationship (3.345 and 3.431 for males and females, respectively). The Gompertz model for weight-at-age data is the same as the one used with length-at-age.

Each model was fitted by non-linear least squares regression, with iterations by the Levenberg-Marquardt algorithm in the STATISTICA 6 software (StatSoft, 2004) and the r^2 value calculated. For each model, growth was estimated for males and females separately and compared using the maximum likelihood test (Kimura, 1980).

Model comparison and selection was based on the small sample corrected form of the Akaike information criterion (AICc) (Shono, 2000), that for the least squares fit can be expressed as:

$$\text{AICc} = \frac{\text{RSS}}{n} + \frac{2k(k+1)}{n-k-1}$$

where RSS is the residual sum of squares, n the number of observations and k is the total number of estimated regression parameters that equals the number of parameters in the model + 1.

The model with the smallest AICc value was selected as the "best" model (AICc, min) and the differences between this "best" model and all others expressed as:

$$\Delta i = \text{AICc}, i - \text{AICc}, \text{min}$$

2.5. Reproductive cycle

Maturity stages were defined for both males and females based on the macroscopic observations of the reproductive organs of the specimens. Males were divided in four stages, where stages 1 and 2 represent immature specimens and stages 3 and 4 represent mature specimens (Table 1). Females were divided in seven stages, where stages 1 and 2 represent immature specimens and stages 3–7 represent mature specimens. In females, stages 1–3 represent the ovarian stages and stages 4–7

Table 1
Macroscopically defined maturity stages for males and females of *Etmopterus pusillus*

Males	
Stage 1: Immature	Underdeveloped and soft claspers, shorter than the pelvic fins. Small whitish threadlike gonads. Sperm duct narrow and straight
Stage 2: Maturing	Claspers developing, longer than the pelvic fins, but still soft. Gonads enlarged. Sperm duct starting to coil
Stage 3: Mature	Claspers fully formed, and stiff. Large and rounded gonads, full of sperm. Sperm ducts coiled
Stage 4: Active	Claspers stiff and swollen. Large and rounded gonads, full of sperm. Sperm flowing under pressure
Females	
Ovarian phases	
Stage 1: Immature	Small ovaries without differentiated oocytes. Uterus threadlike
Stage 2: Maturing	Ovaries a little larger, with oocytes starting to differentiate, but still small in size. Uterus a little wider, but still narrow
Stage 3: Mature	Large ovaries, with large and well differentiated ripe oocytes, orange-yellowish in colour
Uterine phases	
Stage 4: Early pregnancy	Uterus filled with non-segmented and undifferentiated yolky content
Stage 5: Middle pregnancy	Uterus with small embryos, with yolk sacs attached and filled with yolky content
Stage 6: Late pregnancy	Uterus with fully formed embryos, with reduced or inexistent yolk sac
Stage 7: Resting	Ovaries resting with immature oocytes, similar to stage 2. Uterus empty but considerably dilated, sometimes with blood traces from the parturition

the uterine stages (Table 1). In this species, ovarian and uterine phases of mature females are independent and do not occur at the same time. Although no stage 4 females were found, we assume that it is part of this species life cycle given that it has been described for other aplacental viviparous squalid sharks (Clarke et al., 2001; Jakobsdottir, 2001).

The percentage of each maturity stage throughout the year for both males and females was plotted, in order to assess if different stages were occurring predominantly during a specific season or period.

The gonadosomatic index (GSI) and the hepatosomatic index (HSI) were calculated for all specimens and the means for each maturity stage in each sex plotted. These indices were calculated as:

$$\mathrm{GSI} = \frac{\text{gonad weight (g)}}{W_{\mathrm{ev}}\,(\mathrm{g})} \times 100$$

$$\mathrm{HSI} = \frac{\text{liver weight (g)}}{W_{\mathrm{ev}}\,(\mathrm{g})} \times 100$$

Kruskal–Wallis and pairwise Dunn tests were used to test if significant differences occurred between the different maturity stages.

2.6. Maturity

For the purpose of the maturity estimations, the reproductive stages of the specimens were grouped in either mature or immature. Considering that a mature specimen is a specimen that is able to reproduce or has done so in the past (Conrath, 2004), stages 1 and 2 in both males and females were considered immature and the following stages considered mature. Box and whiskers plots were used to plot the means, standard deviations and ranges for both size and age of mature and immature specimens of each sex. A two-way ANOVA was used to test for differences in these mean sizes and ages.

The proportion of mature individuals by 1 cm TL size classes was used to fit length based maturity ogives and to estimate the size at maturity (TL at which 50% of the individuals are mature). The logistic curve was fitted by non-linear least squares regression, using the Levenberg-Marquardt algorithm, in the STATISTICA 6.0 software (StatSoft, 2004) by:

$$P_{L_i} = \frac{1}{1 + \mathrm{e}^{-b(L_i - L_{50})}}$$

where P_{L_i} is the proportion of mature individuals in the size class L_i, b the slope and L_{50} is the size where 50% of the individuals are mature.

The same procedure was followed to estimate age at maturity (age at which 50% of the individuals are mature), using the equation:

$$P_{\mathrm{age}_i} = \frac{1}{1 + \mathrm{e}^{-b(\mathrm{age}_i - \mathrm{age}_{50})}}$$

where P_{age_i} is the proportion of mature individuals in age class age_i, b the slope and age_{50} is the age where 50% of the individuals are mature.

The standard errors and the lower and upper limits of the 95% confidence intervals were calculated for each estimated parameter. Length and age based maturity ogives were fitted to males and females separately, and the maximum likelihood test (Kimura, 1980) used to test for differences between sexes.

Sexual characters such as clasper length in males and uterus width in females were used to confirm the maturity estimated by the ogives. Given that both are paired structures, both the left and the right side structures were measured and compared with ANCOVA tests, using TL as the covariate. Once it was determined that there were no differences between the structures of the two sides, a mean clasper length and uterus width was calculated, respectively, for each male and female and plotted against TL so that relative growth with size of the structure could be observed.

2.7. Fecundity

Total fecundity was estimated by direct methods, by counting both the number of oocytes in mature stage 3 females and the number of mid-term embryos in pregnant females in stage 5. Pregnant females in stage 6, with near-term embryos were not considered for this part of the study, given the possibility that some of the pups may have already been born at the time of capture, resulting in underestimation of fecundity.

3. Results

3.1. Biological sample

A total of 614 specimens (252 females and 362 males) was caught for this study during the sampling period, with 571 specimens caught by the commercial fisheries and 43 specimens caught during the INIAP—IPIMAR research cruise. A subsample of 546 specimens was used for the age and growth study, while for some morphometric relationships 16 additional specimens caught outside the sampled period were also used. Both male and female samples had a wide length range, covering most of the length range described for this species. Females attained slightly larger sizes than males. Specifically, female lengths varied from 15.9 to 50.2 cm TL while males ranged in length from 15.8 to 47.9 cm TL (Fig. 2).

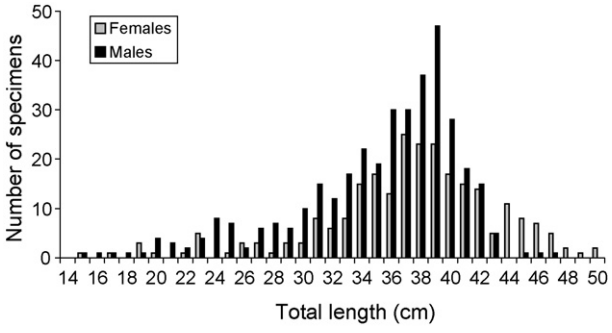

Fig. 2. Size distribution of the sample of *Etmopterus pusillus* used in this study.

Table 2
Linear regressions between TL and FL, PCL, GIR, W and W_{ev} in *Etmopterus pusillus*, indicating the total sample (n), the type of data transformation, the range of the explanatory variable (cm) and the intersect (a) and the slope (b) of the linear regression, with the respective standard errors (S.E.)

Relation	Transf.	Sex	Sample characteristics		Parameters of the relationship				
			n	Range (exp. var.)	a	b	S.E.$_{(a)}$	S.E.$_{(b)}$	r^2
TL-FL	None	Males	288	15.8–46.3	−0.474	0.907	0.131	0.004	0.995
		Females	221	19–50.2	−0.553	0.907	0.153	0.004	0.996
		Combined	509	15.8–50.2	−0.475	0.906	0.098	0.003	0.996
TL-PCL	None	Males	283	15.8–46.3	−0.909	0.825	0.170	0.005	0.991
		Females	215	19–50.2	−1.123	0.828	0.240	0.006	0.988
		Combined	498	15.8–50.2	−0.932	0.825	0.139	0.004	0.989
TL-GIR	None	Males	287	15.8–46.3	−2.834	0.393	0.367	0.010	0.841
		Females	221	19–50.2	−5.098	0.462	0.528	0.014	0.839
TL-W	Nat. log	Males	370	15.8–46.3	−6.793	3.345	0.109	0.031	0.970
		Females	260	15.9–50.2	−7.071	3.431	0.146	0.040	0.966
TL-W_{ev}	Nat. log	Males	369	15.8–46.3	−6.321	3.121	0.096	0.027	0.973
		Females	258	15.9–50.2	−6.500	3.180	0.112	0.031	0.976

The coefficient of determination (r^2) of each regression is also given.

3.2. Morphometric relationships

The morphometric relationships are presented in Table 2. No significant differences between sexes were detected for the TL-FL (ANCOVA: $F = 0.02$; P-value = 0.884) and TL-PCL (ANCOVA: $F = 0.15$; P-value = 0.701) relationships, and therefore regressions for both sexes combined were carried out. For all other regressions significant differences were detected between sexes ($ANCOVA_{TL\text{-}GIR}$: $F = 17.20$; P-value < 0.001; $ANCOVA_{TL\text{-}W}$: $F = 94.52$; P-value < 0.001; $ANCOVA_{TL\text{-}W_{ev}}$: $F = 91.22$; P-value < 0.001).

3.3. Age estimation and validation

There is a clear relation between the growth in weight and size of the spines with TL (Table 3). No differences between sexes were detected for the relations between TL and TSL and between TL and SBW for both the first and the second spines ($ANCOVA_{TL\text{-}TSL1}$: $F < 0.01$; P-value = 0.968; $ANCOVA_{TL\text{-}SBW1}$: $F = 0.65$; P-value = 0.421; $ANCOVA_{TL\text{-}TSL2}$: $F = 0.52$; P-value = 0.470; $ANCOVA_{TL\text{-}SBW2}$: $F = 0.60$; P-value = 0.439), so measurements for both sexes were combined. Differences between sexes were

Table 3
Linear regressions between TL and total spine length (TSL), spine base width (SBW) and spine weight (SW) for both first and second dorsal spines of *Etmopterus pusillus*

Relation	Transf.	Sex	Sample characteristics		Parameters of the relationship				
			n	Range (exp. var.)	a	b	S.E.$_{(a)}$	S.E.$_{(b)}$	r^2
TL-TSL1	None	Males	285	15.8–46.3	0.570	0.489	0.577	0.016	0.764
		Females	196	15.9–48.5	0.837	0.490	0.823	0.022	0.722
		Combined	481	15.8–48.5	0.541	0.494	0.473	0.013	0.752
TL-SBW1	None	Males	289	15.8–47.9	−0.012	0.085	0.118	0.003	0.701
		Females	200	15.9–48.5	−0.056	0.089	0.147	0.004	0.727
		Combined	489	15.8–48.5	−0.079	0.088	0.092	0.003	0.719
TL-SW1	Nat. log.	Males	288	15.8–46.3	−6.520	2.670	0.206	0.058	0.881
		Females	199	15.9–48.5	−6.670	2.725	0.284	0.079	0.859
TL-TSL2	None	Males	308	15.8–47.9	3.222	0.680	0.636	0.018	0.827
		Females	226	15.9–50.2	3.142	0.699	0.813	0.021	0.827
		Combined	534	15.8–50.2	2.825	0.698	0.500	0.014	0.832
TL-SBW2	None	Males	311	15.8–47.9	0.376	0.080	0.113	0.003	0.676
		Females	229	15.9–50.2	0.255	0.084	0.127	0.003	0.738
		Combined	540	15.8–50.2	0.317	0.082	0.083	0.002	0.712
TL-SW2	Nat. log.	Males	310	15.8–46.3	−5.436	2.663	0.170	0.048	0.909
		Females	232	15.9–48.5	−5.387	2.659	0.220	0.061	0.892

The total sample size (n), the type of data transformation, the range of the explanatory variable (cm) and the intersect (a) and the slope (b) of the linear regression, along with the respective standard errors (S.E.) and the coefficient of determination (r^2) of each regression are given.

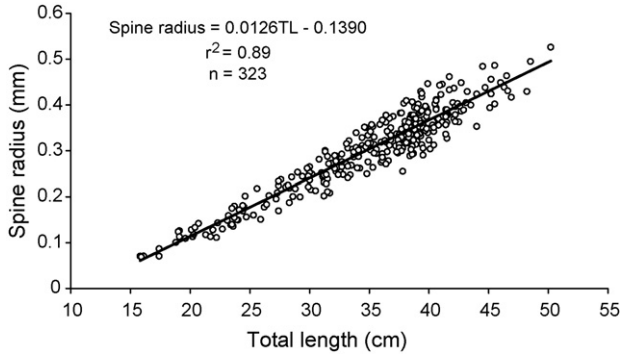

Fig. 3. Relationship between total length of specimens and the radius of the spine sections where age was estimated for both sexes of *Etmopterus pusillus* combined. The regression equation with the respective coefficient of determination (r^2) and the sample size (n) are also given.

detected for both spines for the regressions between TL and SW ($ANCOVA_{TL\text{-}SW1}$: $F = 9.16$; P-value = 0.003; $ANCOVA_{TL\text{-}SW2}$: $F = 8.39$; P-value = 0.004). The relationship between TL and the radius of the spine section where age was estimated was also linear. Given that no differences were detected between males and females (ANCOVA: $F < 0.001$; P-value = 0.945), a regression for both sexes combined was estimated (Fig. 3).

A clear pattern of alternating hyaline and opaque band formation was visible on the spine sections (Fig. 4). Age was determined successfully for 523 of 546 specimens (95.8%), with poor band discrimination (12 specimens) and lack of concordance on at least two of the three readings (11 specimens) accounting for the remainder. The percent of concordant ages in 0, ±1, ±2 and ±3 years was 61.5%, 28.8%, 7.9% and 1.8% for males and 62.9%, 28.8%, 7.6% and 1.5% for females. The APE, V and D precision indices obtained were, respectively, 18.33, 19.79 and 11.43 for males and 11.41, 12.79 and 7.39 for females.

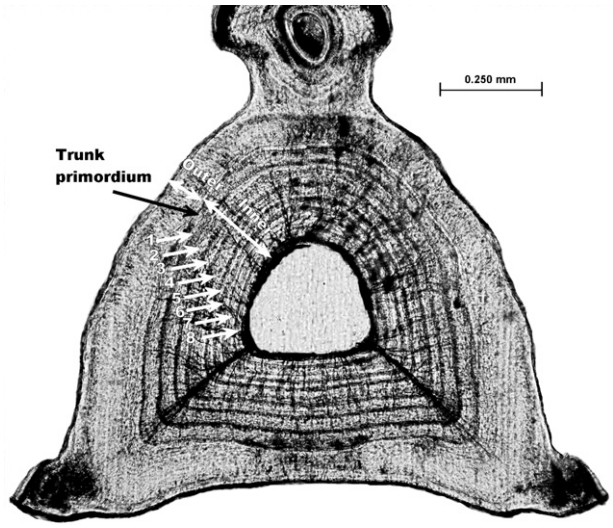

Fig. 4. Microphotograph of a sectioned dorsal spine of a female *Etmopterus pusillus* with 40.4 cm total length and an estimated age of 8 years. It is possible to distinguish the inner trunk layer where the annual bands were counted and the outer trunk layer (without any growth bands and already present in late term embryos), as well as the trunk primordium.

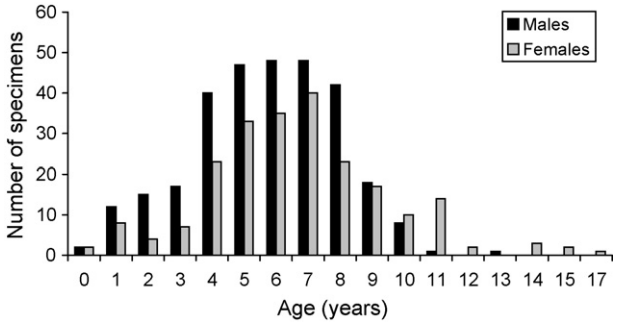

Fig. 5. Age distributions of male and female *Etmopterus pusillus*.

Females had a wider age range than males. Estimated ages of females varied from 0 to 17 years while males ranged from 0 to 13 years. Overall, the female component of this population was older than the male component, since most of the females (87.1%) were between 4 and 11 years old while most of the males (92.0%) were between 2 and 9 years old (Fig. 5). From 1 to 5 years of age there were no significant differences in the mean total length-at-age between sexes, while the older age classes showed significant differences, specifically for age class 5 and age classes 8–10 (Table 4). Differences for older specimens were not tested due to small sample sizes, especially for males.

Age was validated by the marginal increment analysis. There was a clear annual pattern of band formation, with the marginal increment showing progressively higher values from April to November. Between December and March, there was a sharp decrease of the MIR, indicating that the new band is formed during this season of the year. This pattern was visible for all age classes where the MIR was plotted, namely age classes 4, 5, 6, 7 and 8 (Fig. 6). For the other age classes, this type of graph was not plotted due to the low sample size. Statistically significant differences were found between mean MIR values along the different months (ANOVA: $F = 11.48$; P-value < 0.001). The Tukey multiple comparison pairwise test showed that there were differences between only some of the possible pairs of months, specifically between some months with the lowest MIR values (February to March) and the months with the highest MIR values (June to November) (Tukey: P-values < 0.05 in all possible pairwise comparisons). The relatively low January MIR value also differed significantly from the highest MIR values of September and November (Tukey: P-value < 0.05 for all possible pairwise comparisons). No significant differences were detected between the other pairwise comparisons, involving months with mostly intermediate MIR values (Tukey: P-value > 0.05 for all possible pairwise comparisons).

3.4. Growth modelling

All four models gave good fits to the length at age data and produced very similar curves, both in the case of males and females. The VBGF curve with fixed L_0 intersected the YY (total length) axis at values lower than the others where this parameter was estimated (Fig. 7).

For weight based data, the VBGF produced higher estimates of growth throughout the initial age ranges, but from age 10 on

Table 4
Comparison of the mean total length (TL, cm) between male and female *Etmopterus pusillus* for each age group

Age	Females			Males			*t*-Student test		
	n	Mean TL	S.D.	*n*	Mean TL	S.D.	*t*	d.f.	*P*-value
0	2	16.65	1.06	2	15.95	0.21			
1	8	21.35	2.19	12	20.56	1.47	−0.97	18	0.344
2	4	24.26	1.35	15	24.51	0.89	0.45	17	0.658
3	7	28.59	1.85	17	28.00	1.61	−0.78	22	0.445
4	23	32.49	1.91	40	31.64	1.90	−1.70	61	0.094
5	33	35.41	2.01	47	34.47	1.79	−2.20	78	0.030
6	35	37.04	1.59	48	37.06	1.50	0.07	81	0.948
7	40	39.08	1.42	48	38.73	1.10	−1.29	86	0.200
8	23	40.81	1.32	42	40.13	1.21	−2.08	63	0.042
9	17	42.40	1.18	18	41.45	1.10	−2.46	33	0.019
10	10	44.47	1.29	8	42.55	0.72	−3.75	16	<0.01
11	14	45.98	0.81	1	41.50				
12	2	45.90	0.57						
13				1	46.30				
14	3	48.67	1.36						
15	2	48.80	0.85						
16									
17	1	50.20							

n refers to the sample size and S.D. to the standard deviation. The *t*-statistic value, the degrees of freedom (d.f.) and the *P*-value are given.

for males and age 15 on for females there was an inflection and the VBGF estimated lower weights for the same age than the Gompertz model (Fig. 8).

Between sexes comparisons for each length based model showed significant differences between male and female growth curves (Max. Likelihood$_{VBGF}$: $\chi^2 = 52.13$; P-value < 0.05; Max. Likelihood$_{VBGF\ known\ L_0}$: $\chi^2 = 43.36$; P-value < 0.05; Max. Likelihood$_{Logistic}$: $\chi^2 = 47.26$; P-value < 0.05; Max. Likelihood$_{Gompertz}$: $\chi^2 = 47.07$; P-value < 0.05). Between sexes comparisons for each weight based model also showed significant differences between male and female growth curves (Max. Likelihood$_{VBGF}$: $\chi^2 = 161.02$; P-value < 0.05; Max. Likelihood$_{Gompertz}$: $\chi^2 = 157.50$; P-value < 0.05).

For both length at age and weight at age models, females had higher maximum asymptotic sizes and weights and lower growth coefficients than males. For length at age models, the logistic equation produced the lowest maximum asymptotic sizes and the VBGF the highest values, while for weight at age data, the fitted Gompertz model gave higher maximum asymptotic weights than the VBGF for both sexes (Table 5).

For length at age data, all models fitted the data with high values of r^2 and $\Delta i < 2$ for all cases and both sexes. For weight based data, the r^2 values were similar for both models and sexes, but according to the AICc, the Gompertz model was more adequate for males while the VBGF model gave a better fit for females (Table 6).

3.5. Reproductive cycle

The annual variation of the percentage of occurrence of the different maturity stages showed that mature females with ripe oocytes (stage 3) and pregnant females (stages 5 and 6) only

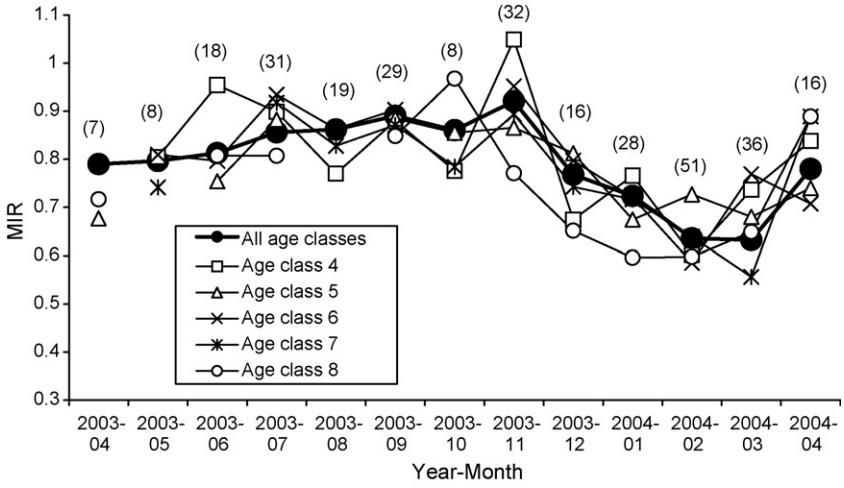

Fig. 6. Monthly evolution of the marginal increment (MIR) both for all age classes combined and for each age class separately. The values in brackets refer to the total sample size (n) in each month.

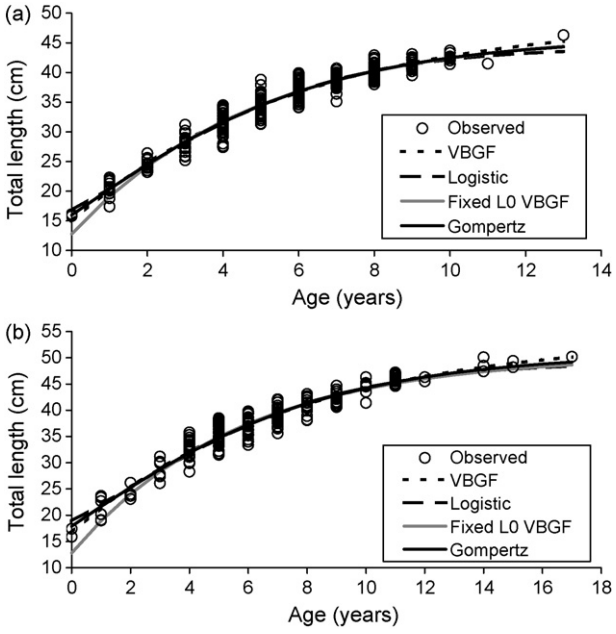

Fig. 7. Length at age data for males (a) and females (b) of *Etmopterus pusillus*, with the respective fitted growth models.

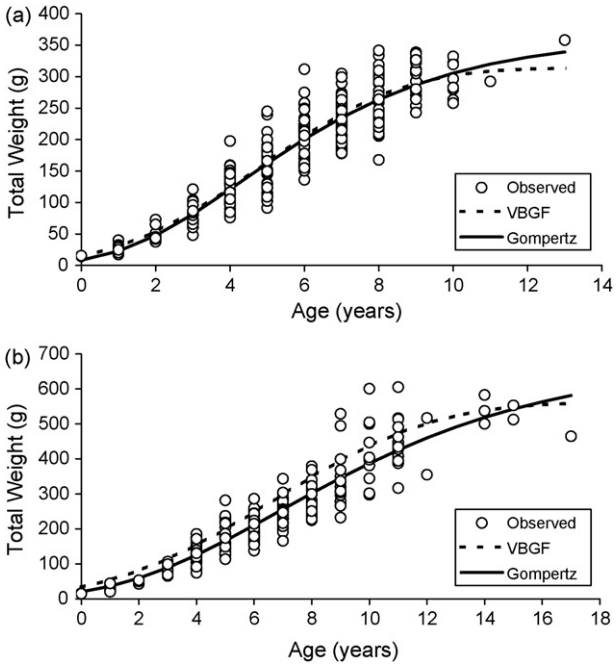

Fig. 8. Weight at age data for males (a) and females (b) of *Etmopterus pusillus*, with the respective fitted growth models.

occurred from November to April. During the rest of the year, only immature specimens (stages 1 and 2) or specimens in the resting phases (stage 7) were caught. In males, all the four stages occurred during the entire year, but the relative percentage of active males (stage 4) was a little higher during August and then from November to April (Fig. 9).

A clear evolution of the GSI was observed as the maturity stages of both males and females developed (Fig. 10). In females, this index is very low while specimens are immature, due to the fact that the gonads have a very low relative weight. In stage 3, this index increases to the highest values, given that during this stage the gonads contain ripe oocytes. In pregnant females, this index falls again to values similar to those of immature specimens, indicating that this species has an alternate reproductive cycle, with the ovarian and the uterine phases occurring at separate times. In this type of reproductive cycle strategy, while females are pregnant the oocytes remain immature and the gonads do not develop, remaining relatively small. In stage 7 females, there is a slight increase of the GSI, probably due to the fact that in some specimens the oocytes are already starting to develop, in order to start a new ovarian cycle. Significant differences were found between the GSI values of the different maturity stages (Kruskal–Wallis: $H = 105.29$, P-value < 0.001). The pairwise Dunn test showed that significant differences occurred between stage 3 and all

Table 5
Comparison of parameters estimated with the different models for length at age and weight at age data, for male and female *Etmopterus pusillus*

Data set	Sex	Model	Maximum asymptotic size				Growth coefficient			
			Estimated	S.E.	Lower 95% CI	Upper 95% CI	Estimated	S.E.	Lower 95% CI	Upper 95% CI
Length at age	Males	VBFG	49.01	0.99	47.07	50.96	0.17	0.01	0.15	0.19
		VBGF Fixed L0	46.81	0.56	45.71	47.91	0.20	0.01	0.19	0.22
		Logistic	44.30	0.47	43.38	45.22	0.35	0.01	0.32	0.38
		Gompertz	45.91	0.62	44.69	47.14	0.26	0.01	0.24	0.29
	Females	VBFG	54.04	1.16	51.75	56.34	0.13	0.01	0.12	0.15
		VBGF Fixed L0	50.51	0.67	49.19	51.83	0.18	0.01	0.16	0.19
		Logistic	49.25	0.65	47.96	50.53	0.27	0.01	0.24	0.29
		Gompertz	50.88	0.80	49.30	52.46	0.20	0.01	0.18	0.22
Weight at age	Males	VBGF	313.77	10.52	293.06	334.47	0.0005	0.0001	0.0003	0.0007
		Gompertz	363.39	18.18	327.60	399.17	0.31	0.03	0.26	0.36
	Females	VBGF	562.21	29.90	503.29	621.13	0.0001	0.0000	0.0000	0.0001
		Gompertz	679.28	54.90	571.08	787.48	0.18	0.02	0.15	0.22

The maximum asymptotic size is indicated in cm for the length at age models and g for the weight at age models. The growth coefficient refers to the parameters k (VBGF models), g (Gompertz model) and r (logistic model).

Table 6
Values of the coefficient of determination (r^2), the small-sample corrected form of Akaike's information criterion (AICc) and the Akaike's differences (Δi) for each growth model, both in length and weight and for each sex

Data set	Sex	Model	r^2	AICc	Δi
Length at age	Males	Gompertz	0.938	2.22	0.00
		Logistic	0.938	2.23	0.01
		VBFG	0.937	2.26	0.03
		VBGF known L_0	0.934	2.33	0.10
	Females	VBFG	0.935	2.69	0.00
		Gompertz	0.933	2.78	0.09
		Logistic	0.929	2.93	0.24
		VBGF known L_0	0.923	3.08	0.39
Weight at age	Males	Gompertz	0.860	961.08	0.00
		VBFG	0.859	963.82	2.74
	Females	VBFG	0.848	2278.93	0.00
		Gompertz	0.845	2321.34	42.42

In each case, models are sorted from best to worst according to the AICc.

others (Dunn: P-values < 0.05), but not between the other possible pair wise combinations (Dunn: P-values > 0.05). In males, there is a progressive increase of this index with the evolution of the maturity stages. Significant differences were found (Kruskal–Wallis: $H = 283.23$; P-value < 0.001), and according to the pair wise multiple comparison test, significant differences occurred between all possible pairs (Dunn: P-values < 0.05 in all cases) except between stages 2 and 3 and between stages 3 and 4 (Dunn: P-values > 0.05).

A clear evolution of HSI is also observed with the evolution of maturity stages in both males and females (Fig. 11). It is possible to observe an increase in this index as females mature until they

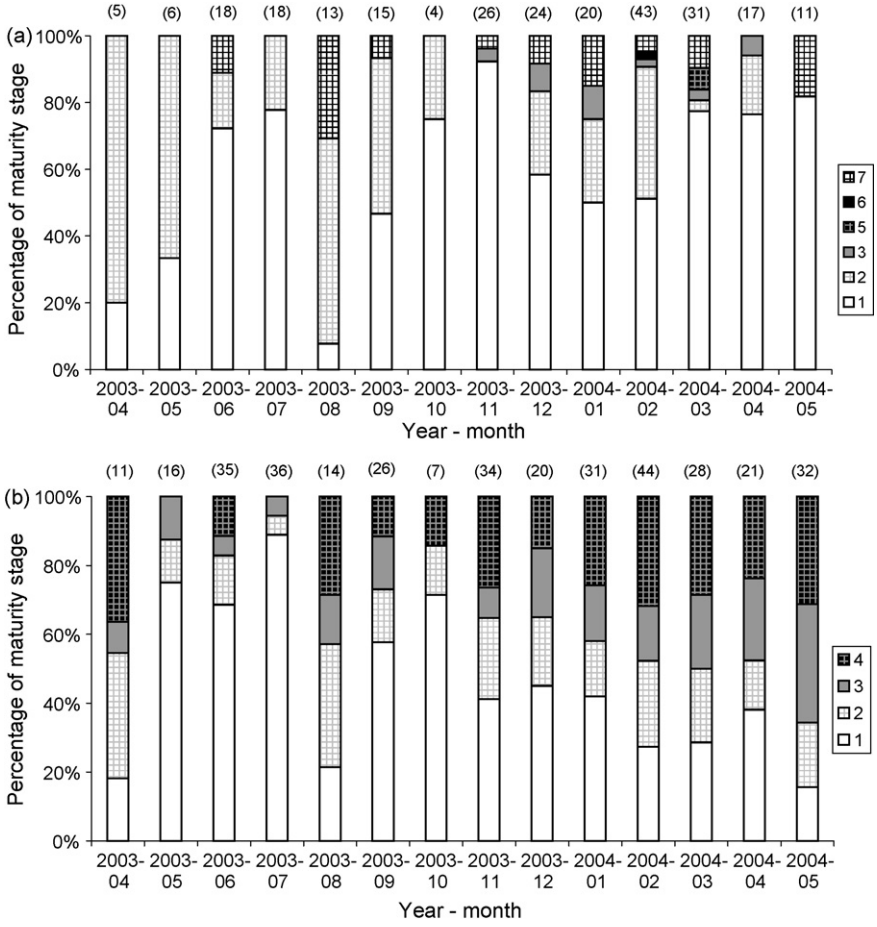

Fig. 9. Annual variation of the percentage of occurrence of the different maturity stages in female (a) and male (b) *Etmopterus pusillus*. The values between brackets are the sample sizes (n).

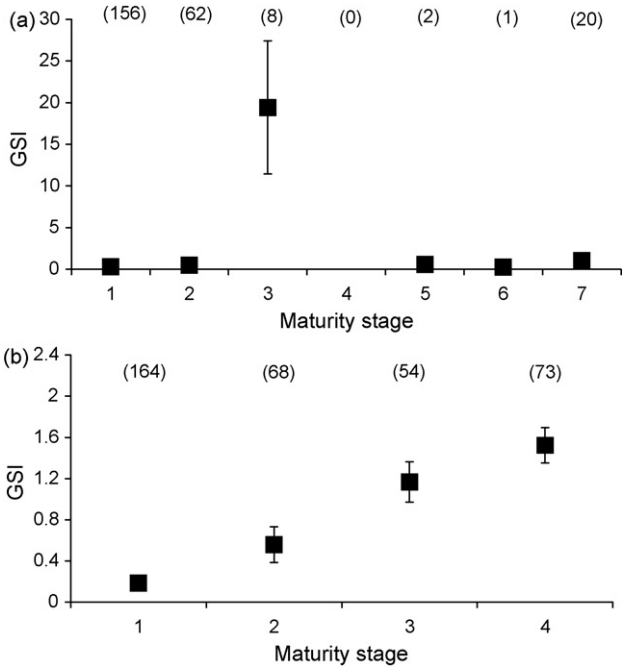

Fig. 10. Evolution of the gonadosomatic index (GSI) for both female (a) and male (b) *Etmopterus pusillus*. Error bars represent ±1 standard deviation. The values above each point are the sample sizes (*n*).

reach stage 3. While females are pregnant there is a decrease in this index, probably due to the high energy demand during this phase. In the resting phase, the index increases again, probably due to fact that the specimens are again starting to accumulate energy for the next reproductive cycle. The variations in HSI were significant (Kruskal–Wallis: $H = 62.40$; P-value < 0.001),

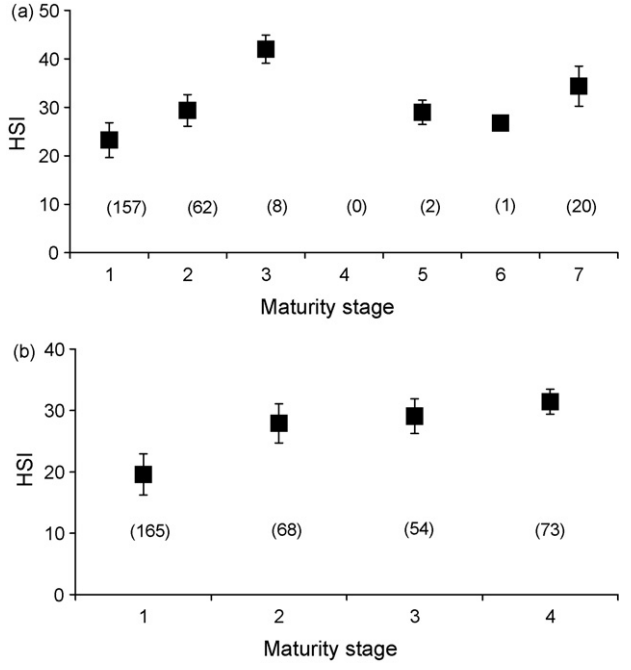

Fig. 11. Evolution of the hepatosomatic index (HSI) for female (a) and male (b) *Etmopterus pusillus*. Error bars represent ±1 standard deviation. The value below each point is the sample size (*n*).

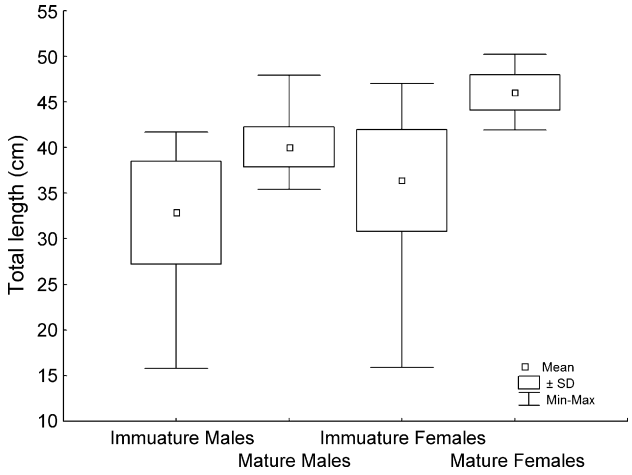

Fig. 12. Box and whiskers plot with the mean, standard deviation and size ranges for mature and immature males and females of *Etmopterus pusillus*.

with the pair wise tests showing differences between stages 1 and 3 and between stages 1 and 7 (Dunn: P-values < 0.05), but not for the other possible pairs (Dunn: P-value > 0.05). In males, there is a progressive increase of the HSI with the evolution of the maturity stage, with the differences more accentuated between stages 1 and 2 and more progressive for the other stages. Significant differences were found (Kruskal–Wallis: $H = 172.07$; P-value < 0.001), with significant differences between all possible pairs (Dunn: P-values < 0.05) except between pairs 2 and 3 and between pairs 3 and 4 (Dunn: P-values > 0.05).

3.6. Maturity

The maximum size of immature males was 41.7 cm while the smallest mature male was 35.4 cm in TL. The largest immature female was 47.0 cm in TL and the smallest mature female had a TL of 41.9 cm (Fig. 12). In terms of age, the oldest immature males were 9 years old and the oldest immature females were 11 years old. On the other hand, the youngest mature males and females were only 5 and 8 years old, respectively (Fig. 13). The two-way ANOVA showed significant differ-

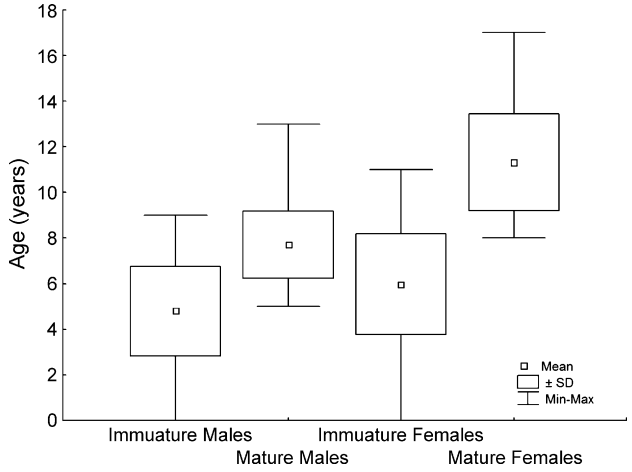

Fig. 13. Box and whiskers plot with the mean, standard deviation and age ranges for mature and immature males and females of *Etmopterus pusillus*.

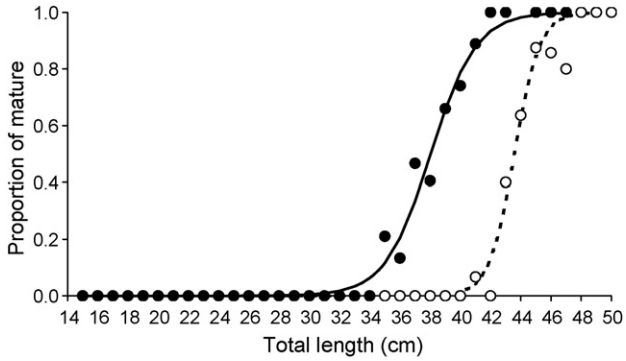

Fig. 14. Size based maturity ogives for *Etmopterus pusillus*. Dark and white points represent the proportion of mature males and females in each 1 cm TL interval class, while the solid and dotted lines represent the corresponding fitted logistic curves.

ences between sexes and for mature or immature condition, for both length (two-way $ANOVA_{Sex}$: $F = 63.77$; P-value < 0.001; two-way $ANOVA_{Maturity}$: $F = 199.49$; P-value < 0.001) and age (two-way $ANOVA_{Sex}$: $F = 103.07$; P-value < 0.001; two-way $ANOVA_{Maturity}$: $F = 305.74$; P-value < 0.001).

Both size based and age based maturity ogives produced good fits to the observed data. The values of r^2 were high; 0.985 and 0.990 for female and male length based ogives and 0.981 and 0.991 for female and male age based ogives.

Females matured at larger sizes than males, with estimated sizes at first maturity of 43.58 cm TL for females and 38.03 cm TL for males (Fig. 14). Females also matured at later ages than males, with estimated ages of first maturity of 7.13 years for males and 9.86 years for females (Fig. 15). There were significant differences between sexes in terms of the parameters of both the size (Max. Likelihood: $\chi^2 = 189.82$; P-value < 0.05) and the age-based (Max. Likelihood: $\chi^2 = 65.01$; P-value < 0.05) maturity ogives.

Since no significant difference was found between left and right side claspers (ANCOVA: $F = 0.10$; P-value $= 0.754$), the mean value was calculated for each specimen and plotted against total length. It is clear that there is a relationship between clasper

Fig. 15. Age based maturity ogives for *Etmopterus pusillus*. Dark and white points represent the proportion of mature males and females in each age class, while the solid and dotted lines represent the corresponding fitted logistic curves.

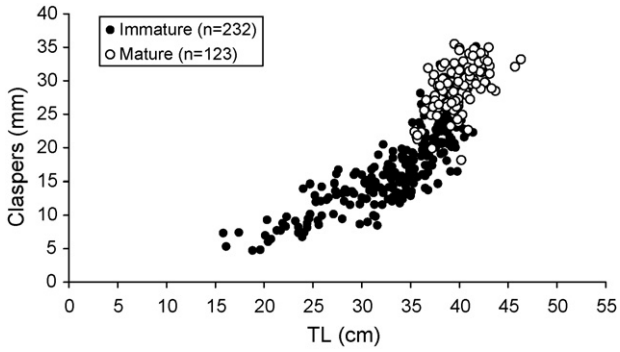

Fig. 16. Relation between total length (TL) and clasper length in males *Etmopterus pusillus*.

length and TL, with an accentuated increase once the specimens achieved maturity (Fig. 16).

Likewise, since there was no significant difference between left and right side uterus (ANCOVA: $F = 0.52$; P-value $= 0.471$), a mean value was calculated for each female and plotted against TL. Although a clear relationship can be observed between uterus width and TL, this relation is not as progressive as that of the claspers in males. In this case, immature specimens have a relatively narrow uterus independently of TL, and once specimens achieved maturity, the uterus either increases substantially (in the case of pregnant females) or remains relatively narrow (mature but not pregnant females) (Fig. 17).

Fifty percent of the females and the males in this population are mature, respectively, at 86.81% and 79.40% of the maximum observed size. In terms of age, 50% of the females are mature at 58.02% and 50% of the males are mature at 54.86% of the maximum observed ages (Table 7).

3.7. Fecundity

The ovarian fecundity in mature (stage 3) females varied from 2 to 18 ripe oocytes, with an average of 10.44 (S.D. = 3.65; $n = 16$), while the uterine fecundity in mid term pregnant females (stage 5) varied from 1 to 6 embryos with an average of 3.50 (S.D. = 3.54; $n = 2$). Only one pregnant female in stage 6 (final pregnancy), with five totally developed and ready to be born embryos was caught.

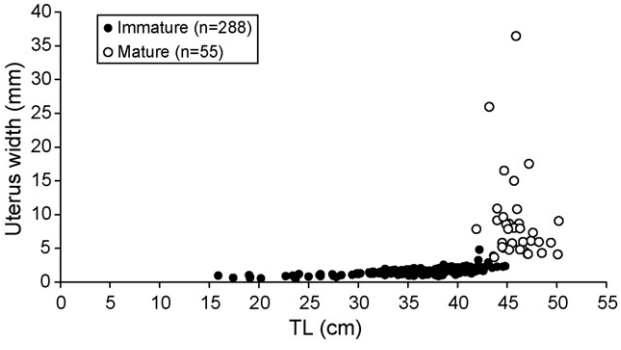

Fig. 17. Relation between total length (TL) and uterus width in females of *Etmopterus pusillus*.

Table 7
Estimated parameters for size (L_{50}) and age (age_{50}) at maturity, with the respective 95% confidence intervals (CI) for males and females of *Etmopterus pusillus*

		Females	Males
Size range (cm)	Immature	15.9–47.0	15.8–41.7
	Mature	41.9–50.2	35.4–47.9
L_{50} (cm)	Estimate	43.58	38.03
	Lower 95% CI	43.38	37.78
	Upper 95% CI	43.78	38.29
Age range (years)	Immature	0–11	0–9
	Mature	8–17	5–13
Age_{50} (years)	Estimate	9.86	7.13
	Lower 95% CI	9.57	6.89
	Upper 95% CI	10.16	7.37
L_{50}/L_{max} (%)		86.81	79.40
Age_{50}/age_{max} (%)		58.02	54.86

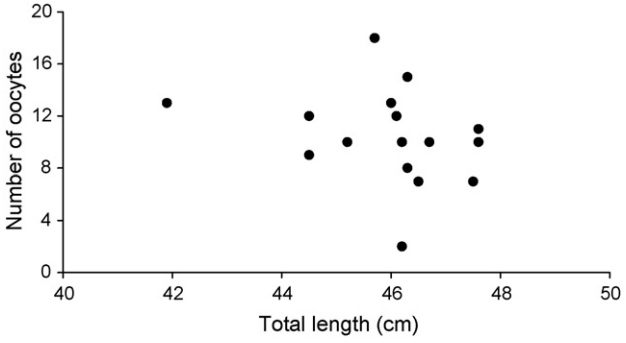

Fig. 18. Relationship between the total length in cm and the number of ripe oocytes present in mature (stage 3) females.

Although the relationship between ovarian fecundity (number of ripe oocytes) and the female TL (ANOVA: $F = 1.05$; P-value = 0.323) (Fig. 18) was not significant, this may be due to the relatively small sample size ($n = 16$) and the very restricted size range of stage 3 females.

4. Discussion

Even though *E. pusillus* is a widespread and at least in some areas very common deep water lantern shark, it has never been thoroughly studied and this is probably the first study to explore aspects of the population biology of this species.

Catches of this species can be very high in the fisheries of the south and south-west coasts of Portugal, and although most of the specimens are discarded, they are returned to sea either dead or with severe injuries that probably affect their survival. Specimens caught with trawls tend to arrive dead on board, probably due to the trauma of being towed for several hours, while specimens caught with longlines are often still alive, but with injuries caused by the hooks and by the sudden changes in pressure and temperature. The survival rates of *Scyliorhinus canicula* discarded by commercial trawlers seems to be very high, ranging from 78% (Rodriguez-Cabello et al., 2005) to 98% (Revill et al., 2005). However, these experiments were conducted in waters much shallower than those where *E. pusillus* is caught and no similar studies are known for *Etmopterus* species. A small survivorship experiment where *E. pusillus* caught by longlines were kept in a temperature controlled tank was carried out during the course of the present study and 100% mortality was achieved within 48 h in all cases, suggesting that the survival of these sharks fished at considerable depths and released at the surface is probably zero. Therefore, alternative by-catch reduction strategies such as the one proposed by Coelho et al. (2003) might be more adequate to prevent excessive fishing related mortality on this species.

The sizes of both males and females caught during this study covered most of the length ranges described for this species (Compagno et al., 2005), so we consider that the sample size and range used were adequate. The fact that different fishing gears were used was an advantage, given that a wide range of depths, and habitats (muddy/sandy habitats fished with trawls and rocky habitats fished with longlines), were sampled. The use of several fishing gears further diminishes the selectivity effect of particular fishing gears that can lead to a skewed distribution of the sample.

As stated by Clarke and Irvine (2006), prior to the examination of growth bands, spine growth should be investigated by measuring spine morphometrics and comparing these with the individual total length. In this work, significant relationships were found between specimen length and several spine morphometrics. Therefore, prior to determination of age, there was already evidence that the growth of spines is proportional to specimen growth and therefore spines could be suitable for estimating age. In addition, relationships between specimen length and spine weight were also investigated and again positive and significant relationships were found, thus confirming the relationship between spine and specimen growth.

During this study, age was estimated based only on the inner dentine layer of the second dorsal spine. The reason for choosing this spine instead of the first dorsal spine is that preliminary investigations showed that the first dorsal spines were often more damaged than the second. This same situation has been observed in other deep water squalid sharks such as *Centroselachus crepidater* in Tasmanian waters (Irvine et al., 2006b), with these authors choosing the second dorsal spine for the same reason. Irvine et al. (2006a) estimated ages of *Etmopterus baxteri* from Tasmanian waters based on both the inner dentine layer and on the exterior bands of the spines, with significant discrepancies found between the two techniques. Irvine et al. (2006a) hypothesized that the inner dentine bands may underestimate age of the older specimens. In the present case, given that the relationship between spine radius, where the dentine is deposited, and specimen growth are linear for the entire length distribution of the species, we do not believe that the deposition of this layer stops in the older specimens. Therefore, only the inner dentine layer was used for age estimation. Nevertheless, future work should also investigate the exterior enamel of the spines.

The validation of age estimates is a fundamental aspect of age and growth studies (Cailliet et al., 1986, 2006; Cailliet, 1990; Campana, 2001; Cailliet and Goldman, 2004). In this study, age estimations were validated by the MIR analysis, which is one of the most commonly used techniques for validating annual

growth band deposition in elasmobranch fishes, including sharks (e.g. Simpfendorfer, 1993; Conrath et al., 2002; Carlson and Baremore, 2005) and rays (e.g. Neer and Thompson, 2005b; Smith et al., 2007).

According to Campana (2001), the MIR analysis is not one of the most accurate for validating ages and this author only classified it in seventh place among 16 possible techniques. However, the techniques that Campana (2001) recommends over the MIR analysis are not applicable to *E. pusillus*. Examples of such techniques are the release of tagged fishes of known age, which implies that the species must be bred in captivity; bomb radiocarbon validation, which implies that at least some specimens must have been born before the 1960's when the ^{14}C in the world oceans increased significantly; or tagging fishes with oxitetracycline, which implies that specimens must be caught, tagged and released without significant mortality. Given that this deep water species can not be bred in captivity, that there are no individuals born before the 1960's and that catch related mortality is high, it is not possible to use capture/tag/recapture or bomb radio-carbon techniques. Thus, we think that MIR analysis is the best available technique for this species.

However, Campana (2001) also recognized that the MIR analysis can be used successfully if some assumptions are respected, namely (1) measuring blindly the structures, without knowledge of the date of capture, (2) observing at least two complete band forming cycles, (3) making an objective interpretation of the results, ideally with the resource of statistics and (4) analysing few age groups at a time. In this work, we effectively respected three of these assumptions, with the only shortcoming being the fact that due to sampling restrictions we analyzed only one instead of two complete cycles. However, given that all other assumptions were respected, we are relatively sure that the age validation procedure used in this study is robust and effectively proves that in this species one pair of bands (one opaque and one hyaline) is formed each year. The only study known at this point where age validation was accomplished for dorsal spines based on bomb radiocarbon is a recent study by Campana et al. (2006) where age was validated for the external enamel bands of *Squalus acanthias*.

Although the von Bertalanffy growth curve is the most widely used to model the growth of fishes (Katsanevakis, 2006), several authors have shown that alternative models can provide better fits to age and growth data for some elasmobranch species. In this study, and even though the VBGF produced good fits and biologically sound results, additional growth curves were used for comparison purposes. Examples of successful alternative growth models applied to elasmobranch fishes include the logistic model applied to the big skate, *Raja binoculata*, the longnose skate, *Raja rhina* (McFarlane and King, 2006) and the spinner shark, *Carcharhinus brevipinna* (Carlson and Baremore, 2005), the Gompertz model applied to the cownose ray, *Rhinoptera bonasus* (Neer and Thompson, 2005b) and the VBGF with known size at birth applied to the bull shark, *Carcharhinus leucas* (Neer and Thompson, 2005a).

The selection of the most adequate model to explain the growth of a species varies between studies. Some authors use the coefficient of determination or parameters such as the lowest mean square error of the regressions as measures of the adequacy of the models (e.g. Carlson and Baremore, 2005). Katsanevakis (2006) suggested the use of the Akaike information criterion (Shono, 2000) as the most efficient model selecting tool and presented several examples where the most adequate model according to this criterion is not always the model with the largest coefficient of determination.

Therefore, the Akaike information criterion was used to evaluate the information that each model was contributing and the Akaike differences used to assess the extent of the contribution of the alternative models. According to Katsanevakis (2006), the lower the value of the Δi the more support an alternative model has, with models with $\Delta i > 10$ having essentially no support, and models with $\Delta i < 2$ having substantial support. In this case, all size at age based models, both in males and females produced values of $\Delta i < 2$, meaning that every model tested in this study fits and can support the data. Although the VBGF with fixed size at birth proved to be the worst model in every case, the Akaike differences were minimal, indicating that the data set had enough small and young specimens, and that the size at birth observed during the surveys and used in this model is probably adequate. For weight at age data, the Gompertz model was the best for male growth while the VBGF model was better for female growth. However, in the case of males, the VBGF model also proved to be relatively good, only exceeding the optimum value of Δi (2) by a small amount, while the Δi value showed no support for the Gompertz model for females.

Even though this is a relatively small species, it is noteworthy that it is long lived and has a relatively slow growth rate. In the only other study on age and growth of another Etmopteridae shark, Irvine et al. (2006a) also reports that the giant lantern shark, *E. baxteri* in Tasmanian waters, is long lived and slow growing. Specifically, Irvine et al. (2006a) reported values of L_{inf} and k of 60.6 and 0.082 for males and 68.1 and 0.040 for females based on the external dorsal spine bands and of 59.6 and 0.163 for males and 69.3 and 0.116 for females based on data from dorsal spine sections.

Since in mature females ovarian stages and uterine stages did not occur at the same time in pregnant females, we can conclude that this species needs a resting phase after parturition, during which the oocytes in the gonads mature for the next cycle. This situation has significant implications for management and conservation, since this species needs two reproductive seasons to complete one reproductive cycle: one season for the development of the oocytes in the gonads followed by one season for the development of the embryos in the uterus. Other deep water squalid sharks have been described to have long gestation periods such as the *Centroscymnus coelolepis* (Clarke et al., 2001), the *Squalus megalops* (Watson and Smale, 1998; Braccini et al., 2006; Hazin et al., 2006) and the *Centrophorus* cf. *uyato* (McLaughlin and Morrissey, 2005).

Uterine reproductive stages were rarely found during this study. Several authors have found similar patterns of rare pregnant females during their surveys and suggestions have been made that pregnant females of some deep water squalids may move into nursery areas, probably in deeper waters, for parturition. This has been hypothesized for *Centroscymnus owstoni* and

C. coelolepis in Japan (Yano and Tanaka, 1988) and *Centroscyllium fabricii* and *Etmopterus princeps* in Iceland (Jakobsdottir, 2001), and we think that a similar situation occurs with *E. pusillus* off southern Portugal.

During this study, it was difficult to establish a definitive reproductive season for *E. pusillus*. It is worth noting that both mature females with ripe oocytes and pregnant females occurred mostly during the winter, specifically from November to April, but the low sample size of both mature and pregnant females may have influenced this analysis. On the other hand, active males were recorded throughout the year, suggesting there is no clearly defined reproductive season. Other authors have found a lack of seasonal reproductive pattern in deep water squalid sharks, including *C. fabricii* and *E. princeps* in Iceland (Jakobsdottir, 2001) and *Etmopterus granulosus* in New Zealand (Wetherbee, 1996). On the other hand, Flammang et al. (2006) found seasonal reproductive patterns in several oviparous deep water Scyliorhinidae sharks, based on gonadosomatic indices variations throughout the year.

E. pusillus in Portuguese waters matures relatively late in its life cycle. Coelho and Erzini (2005) presented preliminary results regarding size at maturity for this species that are very similar to the final results now presented in this work. This information is also now complemented with age at maturity estimates not previously reported. Cortés (2000) examined 164 species of sharks and concluded that on average, maturity occurs at around 75% of the maximum size and around 50% of the maximum age. The values obtained during this study were a little higher, namely 86.81% for females and 79.40% for males for size based data and 58.02% for females and 54.86% for males for age based data. The size at maturity estimated by the maturity ogives resulted in maturity estimates similar to what was observed by the growth of the sexual characters, specifically clasper length in males and the uterus width in females. In this study, females matured at significantly larger sizes and older ages than males. Sexual dimorphism in terms of size-at-maturity is common in elasmobranch fishes, with females usually maturing later and at larger sizes than males. This sexual dimorphism has been described previously for the *Etmopterus* genus by Jakobsdottir (2001) for *E. princeps* and by Irvine et al. (2006a) for *E. baxteri*. Ebert (2005) studied reproductive patterns of several deep water skates along the Bering Sea and concluded that size at maturity occurred at >80% of their TL.

E. pusillus is an aplacental viviparous shark with a relatively low fecundity. The differences observed between the ovarian and the uterine fecundities may be explained by two hypotheses: (1) that part of the ripe oocytes present in stage 3 females never develop into embryos or (2) that since this is an aplacental species, without an umbilical cord connecting the mother to the embryos, it is possible that the stress produced during the fishing process leads to the release of some of the embryos in the uterus of pregnant females. During the sampling process aboard the fishing boats, and while the specimens were deposited in boxes for later processing, it was common to observe middle term embryos in the middle of the catch. This observation supports the second hypothesis, indicating that there is indeed a loss of embryos by pregnant females during the fishing process. Therefore, fecundity in this species should be estimated by the ovarian fecundity and not by uterine fecundity, since the latter may tend to underestimate this parameter.

In this species, no significant relationship was observed between the female total length and the number of ripe oocytes in the gonads. However, we must emphasize that this particular analysis may have been conditioned by the small sample size and the limited size distribution of mature females studied. Other species of deep water viviparous sharks such as *C. owstoni* and *C. coelolepis* in Japan (Yano and Tanaka, 1988) have significant relationships between female size and fecundity. Morphologically, these relationships are sound since in viviparous species the number of oocytes in the gonad, and after fecundation, the number of embryos in the uterus are limited by the size of the abdominal cavity, which increases with increasing specimen size.

In conclusion, this study suggests that *E. pusillus* in the NE Atlantic has a vulnerable life cycle, a situation previously described for several other deep water squalids. Several deep water fisheries operate in the area and there are no perspectives of a decrease of effort or a reduction of the discards in the near future. Even if effective management and conservation plans are implemented for deep water shark species in the future, discarded species such as *E. pusillus*, where accurate catch data is extremely difficult to obtain, will still remain a problem for management and conservation.

Acknowledgments

This study was funded by POCI 2010 (Programa Operacional Ciência e Inovação 2010) and FSE (Fundo Social Europeu) through a FCT (Foundation for Science and Technology) Ph.D. grant (Ref. SFRH/BD/10357/2002). The authors are grateful to all fishermen who collaborated in collecting specimens for this study. Special thanks go to Ilídio Diogo and Francisco Diogo, skippers of the longliner "Branca de Sagres" and Helder Cavaco, skipper of the bottom trawler "Gamba". The authors wish to thank Dr. Ivone Figueiredo and Dr. Pedro Bordalo Machado (INIAP—IPIMAR) for providing the samples collected during this institute's annual demersal trawl survey.

References

Beamish, R.J., Fournier, D.A., 1981. A method for comparing the precision of a set of age determinations. Can. J. Fish. Aquat. Sci. 38, 982–983.

Braccini, J.M., Gillanders, B.M., Walker, T.I., 2006. Determining reproductive parameters for population assessments of chondrichthyan species with asynchronus ovulation and parturition: piked spurdog (*Squalus megalops*) as a case study. Mar. Freshwater Res. 57, 105–119.

Cailliet, G.M., 1990. Elasmobranch age determination and verification: an updated review. In: Pratt, W.S., Gruber, S.H., Taniuchi, T. (Eds.), Elasmobranchs as Living Resources: Advances in the Biology, Ecology, Systematics, and the Status of the Fisheries. NOAA Tech. Rep. 90, pp. 157–165.

Cailliet, G.M., Goldman, K.J., 2004. Age determination and validation in Chondrichthyan fishes. In: Carrier, J., Musick, J.A., Heithaus, M.R. (Eds.), Biology of Sharks and Their Relatives. CRC Press, Boca Raton, pp. 399–447.

Cailliet, G.M., Radtke, R.L., Welden, B.A., 1986. Elasmobranch age determination and verification: a review. In: Uyeno, T., Arai, R., Taniuchi, T., Matsuura,

K. (Eds.), Indo Pacific Fish Biology. Proceedings of the second international conference on Indo Pacific fishes, Tokyo National Museum, Ueno Park, Tokyo, pp. 345–360.

Cailliet, G.M., Smith, W.D., Mollet, H.F., Goldman, K.J., 2006. Age and growth studies of chondrichthyan fishes: the need for consistency in terminology, verification, validation, and growth function fitting. Environ. Biol. Fishes 77, 211–228.

Campana, S.E., 2001. Accuracy, precision and quality control in age determination, including a review of the use and abuse of age validation methods. J. Fish Biol. 59, 197–242.

Campana, S.E., Jones, C., McFarlane, G.A., Myklevoll, S., 2006. Bomb dating and age validation using the spines of spiny dogfish (*Squalus acanthias*). Environ. Biol. Fishes 77, 327–336.

Carlson, J.K., Baremore, I.E., 2005. Growth dynamics of the spinner shark (*Carcharhinus brevipinna*) off the United States southeast and Gulf of Mexico coasts: a comparison of methods. Fish. Bull. 103, 280–291.

Chang, W.Y.B., 1982. A statistical method for evaluating the reproducibility of age determinations. Can. J. Fish. Aquat. Sci. 39, 1208–1210.

Clarke, M.W., Connolly, P.L., Bracken, J.J., 2001. Aspects of reproduction of the deep water sharks *Centroscymnus coelolepis* and *Centrophorus squamosus* from west of Ireland and Scotland. J. Mar. Biol. Ass. U.K. 81, 1019–1029.

Clarke, M.W., Irvine, S.B., 2006. Terminology for the ageing of chondrichthyan fish using dorsal-fin spines. Environ. Biol. Fishes 77, 273–277.

Coelho, R., Erzini, K., 2005. Length at first maturity of two species of lantern sharks (*Etmopterus spinax* and *Etmopterus pusillus*) of southern Portugal. J. Mar. Biol. Ass. U.K. 85, 1163–1165.

Coelho, R., Bentes, L., Gonçalves, J.M.S., Lino, P.G., Ribeiro, J., Erzini, K., 2003. Reduction of elasmobranch by-catch in the hake semipelagic near-bottom longline fishery in the Algarve (Southern Portugal). Fish. Sci. 69, 293–299.

Coelho, R., Erzini, K., Bentes, L., Correia, C., Lino, P.G., Monteiro, P., Ribeiro, J., Gonçalves, J.M.S., 2005. Semi-pelagic longline and trammel net elasmobranch catches in Southern Portugal: catch composition, catch rates and discards. J. Northw. Atl. Fish. Sci. 35, 531–537.

Compagno, L.J.V., 1984. Sharks of the World. An Annotated and Illustrated Catalogue of Shark Species Known to Date. Part 2. Carcharhiniformes. FAO, Rome.

Compagno, L.J.V., Dando, M., Fowler, S., 2005. Sharks of the World. Collins, London.

Conrath, C.L., 2004. Reproductive biology. In: Musick, J.A., Bonfil, R. (Eds.), Elasmobranch Fisheries Management Techniques. Asia-Pacific Economic Cooperation, Singapore, pp. 133–164.

Conrath, C.L., Gelsleichter, J., Musick, J.A., 2002. Age and growth of the smooth dogfish (*Mustelus canis*) in the northwest Atlantic Ocean. Fish. Bull. 100, 674–682.

Cortés, E., 2000. Life history patterns and correlations in sharks. Rev. Fish. Sci. 8, 299–344.

Ebert, D.A., 2005. Reproductive biology of skates, *Bathyraja* (Ishiyama), along the eastern Bering Sea Continental Slope. J. Fish Biol. 66, 618–649.

Flammang, B.E., Ebert, D.A., Cailliet, G.M., 2006. Reproductive biology of deep-sea catsharks (Chondrichthyes: Scyliorhinidae) in the eastern North Pacific. Environ. Biol. Fish., 15, 007/s10641-006-9162-9.

Fowler, S.L., Cavanagh, R.D., Camhi, M., Burgess, G.H., Cailliet, G.M., Fordham, S.V., Simpfendorfer, C.A., Musick, J.A., 2005. Sharks, Rays and Chimaeras: The Status of the Chondrichthyan Fishes. IUCN, Gland, Switzerland and Cambridge.

Hazin, F.H.V., Fischer, A.F., Broadhurst, M.K., Veras, D., Oliveira, P.G., Burgess, G.H., 2006. Notes on the reproduction of *Squalus megalops* off northeastern Brazil. Fish. Res. 79, 251–257.

Irvine, S.B., Stevens, J.D., Laurenson, L.J.B., 2006a. Comparing external and internal dorsal-spine bands to interpret the age and growth of the giant lantern shark, *Etmopterus baxteri* (Squaliformes: Etmopteridae). Environ. Biol. Fishes 77, 253–264.

Irvine, S.B., Stevens, J.D., Laurenson, L.J.B., 2006b. Surface bands on deepwater squalid dorsal-fin spines: an alternative method for ageing *Centroselachus crepidater*. Can. J. Fish. Aquat. Sci. 63, 617–627.

Jakobsdottir, K.B., 2001. Biological aspects of two deep-water squalid sharks: *Centroscyllium fabricii* (Reinhardt, 1825) and *Etmopterus princeps* (Collett, 1904) in Icelandic waters. Fish. Res. 51, 247–265.

Katsanevakis, S., 2006. Modelling fish growth: model selection, multi-model inference and model selection uncertainty. Fish. Res. 81, 229–235.

Kimura, D.K., 1980. Likelihood methods for the von Bertalanffy growth curve. Fish. Bull. 77, 765–776.

LaMarca, M.S., 1966. A simple technique for demonstrating calcified annuli in the vertebrae of large elasmobranchs. Copeia 2, 351–352.

McFarlane, G.A., King, J.R., 2006. Age and growth of big skate (*Raja binoculata*) and longnose skate (*Raja rhina*) in British Columbia waters. Fish. Res. 78, 169–178.

McLaughlin, D.M., Morrissey, J.F., 2005. Reproductive biology of *Centrophorus* cf. *uyato* from the Cayman Trench, Jamaica. J. Mar. Biol. Ass. U.K. 85, 1185–1192.

Monteiro, P., Araujo, A., Erzini, K., Castro, M., 2001. Discards of the Algarve (southern Portugal) crustacean trawl fishery. Hydrobiologia 449, 267–277.

Neer, J.A., Thompson, B.A., 2005a. Age and growth of *Carcharhinus leucas* in the northern Gulf of Mexico: incorporating variability in size at birth. J. Fish Biol. 67, 370–383.

Neer, J.A., Thompson, B.A., 2005b. Life history of the cownose ray, *Rhinoptera bonasus*, in the northern Gulf of Mexico, with comments on geographic variability in life history traits. Environ. Biol. Fishes 73, 321–331.

Revill, A.S., Dulvy, N.K., Holst, R., 2005. The survival of discarded lesser-spotted dogfish (*Scyliorhinus canicula*) in the Western English Channel beam trawl fishery. Fish. Res. 71, 121–124.

Rodriguez-Cabello, C., Fernandez, A., Olaso, I., Sanchez, F., 2005. Survival of small-spotted catshark (*Scyliorhinus canicula*) discarded by trawlers in the Cantabrian Sea. J. Mar. Biol. Ass. U.K. 85, 1145–1150.

Saldanha, L., 1997. Fauna Submarina Atlântica. Publicações Europa América, Mem Martins.

Shono, H., 2000. Efficiency of the finite correction of Akaike's information criteria. Fish. Sci. 66, 608–610.

Simpfendorfer, C.A., 1993. Age and growth of the Australian sharpnose shark, *Rhizoprionodon taylori*, from North Queensland, Australia. Environ. Biol. Fishes 36, 233–241.

Smith, W.D., Cailliet, G.M., Melendez, E.M., 2007. Maturity and growth characteristics of a commercially exploited stingray, *Dasyatis dipterura*. Mar. Freshwater Res. 58, 54–66.

StatSoft, 2004. Electronic Statistics Textbook. StatSoft, Tulsa.

Watson, G., Smale, M.J., 1998. Reproductive biology of shortnose spiny dogfish, *Squalus megalops*, from the Agulhas Bank, South Africa. Mar. Freshwater Res. 49, 695–703.

Wetherbee, B.M., 1996. Distribution and reproduction of the southern lantern shark from New Zealand. J. Fish Biol. 49, 1186–1196.

Yano, K., Tanaka, S., 1988. Size at maturity, reproductive cycle, fecundity, and depth segregation of the deep sea squaloid sharks *Centroscymnus owstoni* and *C. coelolepis* in Suruga Bay, Japan. Bull. Jpn. Soc. Sci. Fish. 54, 167–174.